JCB Article

Cortactin is necessary for E-cadherin–mediated contact formation and actin reorganization

Falak M. Helwani,[1] Eva M. Kovacs,[2] Andrew D. Paterson,[2] Suzie Verma,[1,2] Radiya G. Ali,[2] Alan S. Fanning,[3] Scott A. Weed,[4] and Alpha S. Yap[1,2]

[1]Division of Molecular Cell Biology, Institute for Molecular Bioscience, and [2]School of Biomedical Science, University of Queensland, Brisbane, Queensland 4072, Australia
[3]Department of Cell and Molecular Physiology, University of North Carolina at Chapel Hill, Chapel Hill, NC 27599
[4]Department of Craniofacial Biology, University of Colorado Health Sciences Center, Denver, CO 80262

Classical cadherin adhesion molecules are key determinants of cell–cell recognition during development and in post-embryonic life. A decisive step in productive cadherin-based recognition is the conversion of nascent adhesions into stable zones of contact. It is increasingly clear that such contact zone extension entails active cooperation between cadherin adhesion and the force-generating capacity of the actin cytoskeleton. Cortactin has recently emerged as an important regulator of actin dynamics in several forms of cell motility. We now report that cortactin is recruited to cell–cell adhesive contacts in response to homophilic cadherin ligation. Notably, cortactin accumulates preferentially, with Arp2/3, at cell margins where adhesive contacts are being extended. Recruitment of cortactin is accompanied by a ligation-dependent biochemical interaction between cortactin and the cadherin adhesive complex. Inhibition of cortactin activity in cells blocked Arp2/3-dependent actin assembly at cadherin adhesive contacts, significantly reduced cadherin adhesive contact zone extension, and perturbed both cell morphology and junctional accumulation of cadherins in polarized epithelia. Together, our findings identify a necessary role for cortactin in the cadherin–actin cooperation that supports productive contact formation.

Introduction

Classical cadherin adhesion molecules are fundamental regulators of tissue organization in metazoan organisms (Takeichi, 1991; Yap et al., 1997). One key function of these proteins is to mediate adhesive recognition between motile cells during tissue patterning. As exemplified by E-cadherin, this characteristically entails a morphological process where limited initial points of cell–cell contact become progressively extended into stable zones of adhesion (contact zone extension; Adams et al., 1998; Vasioukhin et al., 2000; Ehrlich et al., 2002). However, productive contact zone extension is not solely determined by the surface adhesive properties of cadherins. Contact formation also involves intimate functional cooperation between cadherins and the actin cytoskeleton (Adams and Nelson, 1998; Vasioukhin et al., 2000). Of note, it has recently become apparent that cadherin adhesions can mark sites for actin assembly. This cooperation may serve both to initially appose cell surfaces (Vasioukhin et al., 2000; Vaezi et al., 2002) and to productively extend contacts after initial adhesion is made (Ehrlich et al., 2002; Kovacs et al., 2002b).

The molecular mechanisms that link cadherins and actin assembly are now beginning to be identified. One such mechanism is likely to involve interaction between E-cadherin and the Arp2/3 actin nucleator complex. Recently, we found that cadherin adhesive ligation can recruit the Arp2/3 complex to the cell surface (Kovacs et al., 2002b). Strikingly, Arp2/3 preferentially localizes to sites of actin assembly in newly forming cadherin contacts. Such cadherin-directed localization of Arp2/3 provides an attractive potential mechanism to optimally focus the polymerization of actin in newly forming contacts, thereby allowing its force-generating capacity to be concentrated to drive the extension of those contacts.

The molecules that regulate actin assembly at cadherin contacts remain to be elucidated. Cortactin has recently

F.M. Helwani and E.M. Kovacs contributed equally to this paper.

The online version of this article includes supplemental material.

Address correspondence to Alpha S. Yap, Institute for Molecular Bioscience, University of Queensland, St. Lucia, Brisbane, Queensland 4072, Australia. Tel.: 61-7-3346-2013. Fax: 61-7-3346-2101. email: a.yap@mailbox.uq.edu.au

Key words: E-cadherin; cortactin; actin assembly; Arp2/3; epithelia

Abbreviations used in this paper: hE-CHO, CHO cell stably transfected with human E-cadherin; hE/Fc, human E-cadherin fused to the Fc region of IgG; NTA, NH_2-terminal acidic; RNAi, RNA interference; TIRF, total internal reflection fluorescence.

© The Rockefeller University Press, 0021-9525/2004/03/899/12 $8.00

emerged as a potentially critical regulator of actin assembly in a variety of contexts that entail dynamic control of membrane movements (Olazabal and Machesky, 2001; Weed and Parsons, 2001; Higgs, 2002). First discovered as an src-kinase substrate in RSV-transformed fibroblasts (Wu et al., 1991), cortactin is a multidomain actin-binding protein (Wu and Parsons, 1993; Weed and Parsons, 2001). Cortactin can interact directly with both Arp2/3 (via an NH_2-terminal acidic [NTA] domain) and F-actin (notably via the fourth of six tandem repeats located in the NH_2-terminal half of the molecule; Weed et al., 2000). Direct binding of cortactin activates Arp2/3-driven actin nucleation (Uruno et al., 2001; Weaver et al., 2001, 2002), and this is enhanced when WASp-interacting protein associates with the cortactin SH3 domain (Kinley et al., 2003). Cortactin also inhibits disassembly of Arp2/3-generated actin filaments, an effect that can potentially stabilize the cortical actin network (Weaver et al., 2001). These properties of cortactin prompted us to examine its role in cadherin contact formation. We now report that cortactin is necessary for cadherin-directed actin assembly and contact zone extension.

Results

E-cadherin ligation is sufficient to recruit cortactin to the cell surface

The capacity for cortactin to participate in cadherin function was first suggested by its immunofluorescent localization in cultured cell monolayers that contain endogenous E-cadherin. MDCK (Fig. 1, untreated), as well as NMuMG and MCF-7 cells (unpublished data), displayed extensive cortactin staining in cadherin-based cell–cell contacts. Moreover, cortactin was rapidly recruited to MDCK cell–cell contacts as cadherin adhesion was restored after being disrupted by chelation of extracellular calcium (Fig. 1). However, cortactin did not always precisely colocalize with E-cadherin, typically being distributed somewhat less continuously than E-cadherin in cell–cell contacts. Cortactin also showed vesicular and perinuclear staining, consistent with a reported role in cellular trafficking (Kaksonen et al., 2000; Lynch et al., 2003). These data suggested that cortactin could be rapidly recruited to newly forming cadherin contacts.

To determine if cadherin adhesion was responsible for recruiting cortactin to cell–cell contacts, we first compared the localization of cortactin in CHO cells stably transfected with human E-cadherin (hE-CHO cells). Parental CHO cells, which do not express detectable classical cadherins (Kovacs et al., 2002b), formed loose contacts with one another as detected by phalloidin staining (Fig. 2 A), but these did not accumulate cortactin. In contrast, cortactin frequently concentrated with E-cadherin in contacts between hE-CHO cells (Fig. 2 A). Like MDCK cells, cortactin staining was often less extensive than the cadherin staining.

Then, we used a dimeric recombinant ligand containing the complete ectodomain of human E-cadherin fused to the Fc region of IgG (hE/Fc) to test if cadherin homophilic adhesion was sufficient to recruit cortactin to the plasma membrane (Fig. 2 B). This and similar reagents (Noren et al., 2001; Lambert et al., 2002) support adhesion and cadherin-activated cell signaling (Noren et al., 2001; Kovacs et al., 2002a,b). Latex beads coated with hE/Fc attached efficiently to the dorsal surfaces of hE-CHO cells, thereby providing spatially defined adhesive signals (Goodwin et al., 2003). Prominent cortactin accumulation was detected at the sites of bead binding (Fig. 2 B), where it colocalized with β-catenin (marking the cellular cadherin complex). In contrast, neither cortactin nor β-catenin (unpublished data) accumulated at sites of contact between cells and Con A–coated beads, despite effective binding of beads to cell surfaces (Fig. 2 B). Although 95% of hE/Fc-coated beads ($n = 40$) recruited cort-

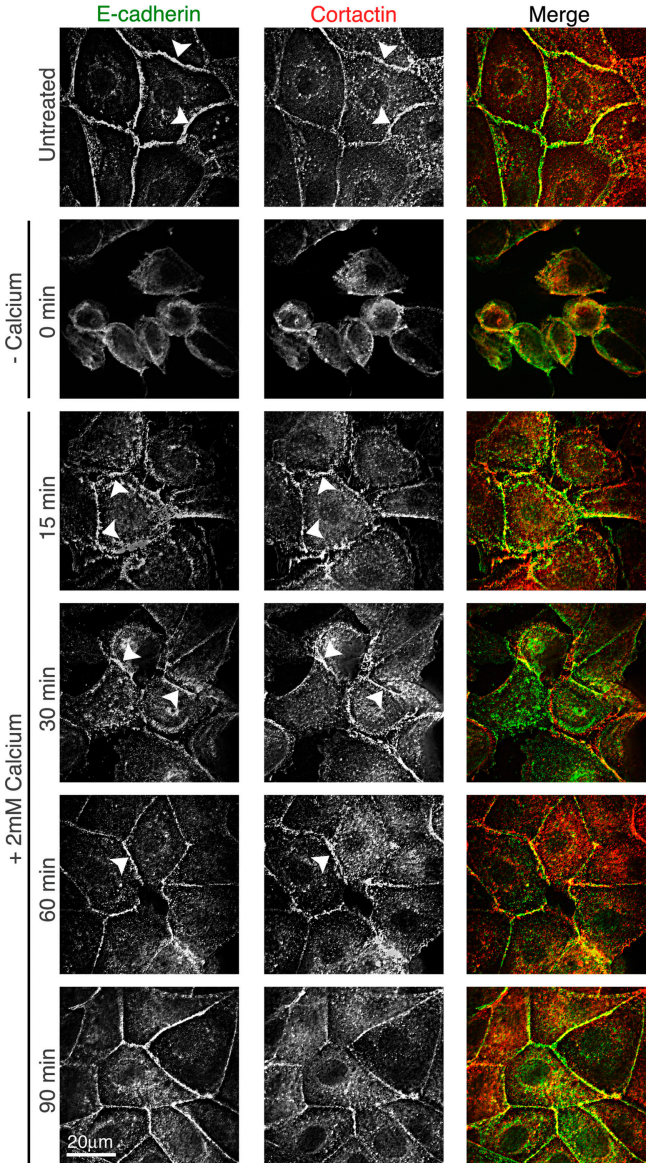

Figure 1. **Cortactin localizes to cadherin-based cell–cell contacts.** MDCK cell monolayers were fixed at confluence (untreated), immediately after incubation with 2 mM EGTA (0 min), or 15–90 min after replenishment of 2 mM extracellular calcium. Cortactin staining was identified in many cell–cell contacts that also contained E-cadherin (arrowheads). Both E-cadherin and cortactin staining were lost from cell peripheries when contacts were disrupted upon chelation of extracellular calcium, but rapidly returned as contacts reformed upon restoration of extracellular calcium. Epi-illumination fluorescence images were processed by three-dimensional blind deconvolution from z-axis stacks.

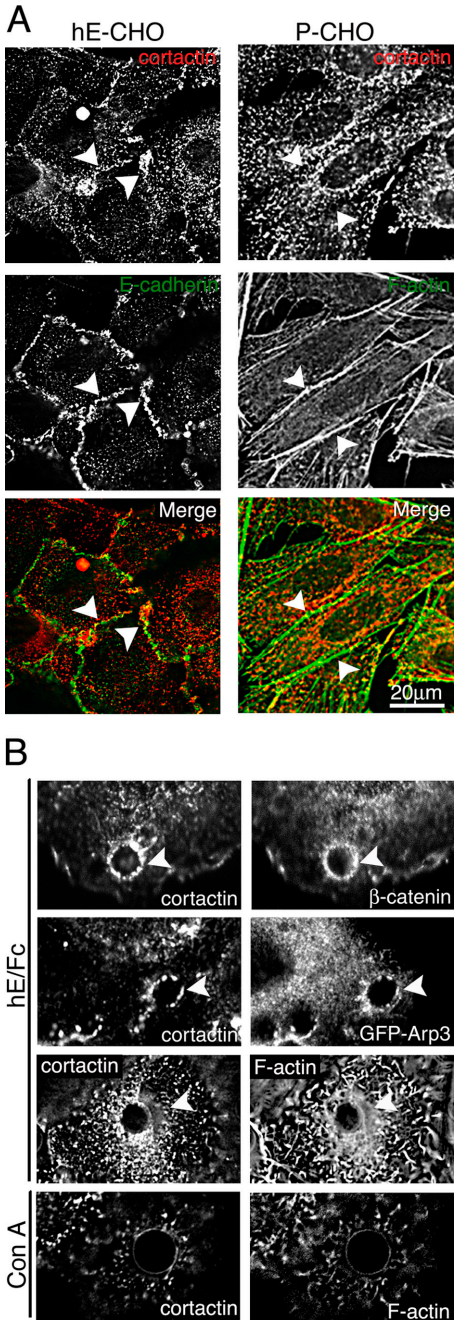

Figure 2. **E-cadherin homophilic ligation is sufficient to recruit cortactin to adhesive contacts.** (A) E-cadherin is necessary to recruit cortactin to cell–cell contacts. CHO cells stably expressing human E-cadherin (hE-CHO) and parental CHO cells (P-CHO) were grown in monolayer culture, then immunostained for cortactin and either E-cadherin (hE-CHO cells) or fluorescently labeled phalloidin (P-CHO cells) to identify the cell–cell contacts (marked by arrowheads). Cortactin was observed in cell–cell contacts between hE-CHO cells, but not between P-CHO cells. Epi-illumination images were processed by three-dimensional deconvolution. (B) Cortactin is recruited to localized sites of cadherin homophilic ligation. 6-μm-diam latex beads coated with hE/Fc (arrowheads) or Con A were allowed to adhere to the dorsal surfaces of hE-CHO cells for 90 min, and were immunostained for cortactin and β-catenin (marking the cadherin–catenin complex), transiently expressed GFP-Arp3, or F-actin (phalloidin). Beads were visualized by laser-scanning confocal microscopy. Con A beads are identified by their autofluorescent outlines.

actin, only 5% of Con A–coated beads ($n = 40$) showed any cortactin staining. This suggested that homophilic cadherin binding sufficed to recruit cortactin to sites of adhesion.

Cortactin accumulates preferentially at the extending margins of cadherin adhesive contact zones

To better define the precise pattern of cortactin recruitment in cadherin contacts, we used total internal reflection fluorescence (TIRF) microscopy to visualize cortactin in cells adherent to hE/Fc-coated substrata (Fig. 3). In this assay, the cell–substratum interface constitutes the zone of contact and, as cells adhere, they progressively extend their zones of contact by protruding cadherin-based lamellipodia (Fig. 3 and Video 1, available at http://www.jcb.org/cgi/content/full/jcb.200309034/DC1; Kovacs et al., 2002a,b). Although not designed to reproduce all events likely to arise when native cell surfaces are brought together, these planar spreading assays have the analytic advantage of allowing us to isolate dynamic cellular events that arise as specific responses to cadherin ligation, independent of any potential juxtacrine signals (Noren et al., 2001; Kovacs et al., 2002a,b; Yap and Kovacs, 2003). Moreover, many salient features displayed by cells in these assays, including the spatial confinement of Rac and PI3-kinase signaling to the outer, extending margins of the contact (Kovacs et al., 2002a), are also observed when migrating MDCK cells establish productive contacts with one another (Ehrlich et al., 2002). Combined with the ability of TIRF microscopy to image molecules located within 100 nm of the cell substrate boundary (Steyer and Almers, 2001), these assays thus provided the opportunity to examine dynamic events located at the cadherin adhesive interface itself.

TIRF microscopy of hE-CHO cells adherent to hE/Fc-coated substrata revealed that cortactin stained in prominent bands at the very outer margins of the contact zones (Fig. 3, A and A′). This confirmed that the concentration of staining at outer margins identified by confocal microscopy (Fig. 4) reflects its localization at the contact interface itself. As seen in monolayers, cortactin also stained in the perinuclear region as well as in puncta throughout the bases of lamellipodia. In contrast, relatively little cortactin staining was seen in the bodies of the lamellipodia proximal to the outer margins (Fig. 3 A′). However, by TIRF illumination, β-catenin (marking the cadherin complex) distributed diffusely in clusters throughout the lamellipodia (Fig. 3, B and B′) and contact zones generally (Fig. 3 B). Therefore, the accumulation of cortactin at the outer margins, and its relative paucity immediately proximal to the margins, was not due to changes in the proximity of the cell membrane to the adhesive substratum.

The prominent localization of cortactin at the outer margins was noteworthy because these outer margins represent regions where the zones of contact are being actively extended and remodeled. Indeed, time-lapse TIRF imaging of transiently transfected hE-CHO cells further revealed that GFP-cortactin rapidly accumulated at the outer margins of lamellipodia as cells extended their contacts on hE/Fc-substrata (Fig. 3 C; Video 1). Characteristically, GFP-cortactin appeared to consistently accumulate wherever the outer margin was extended. Again, despite increased perinuclear and cytoplasmic fluorescence due to transient expression of

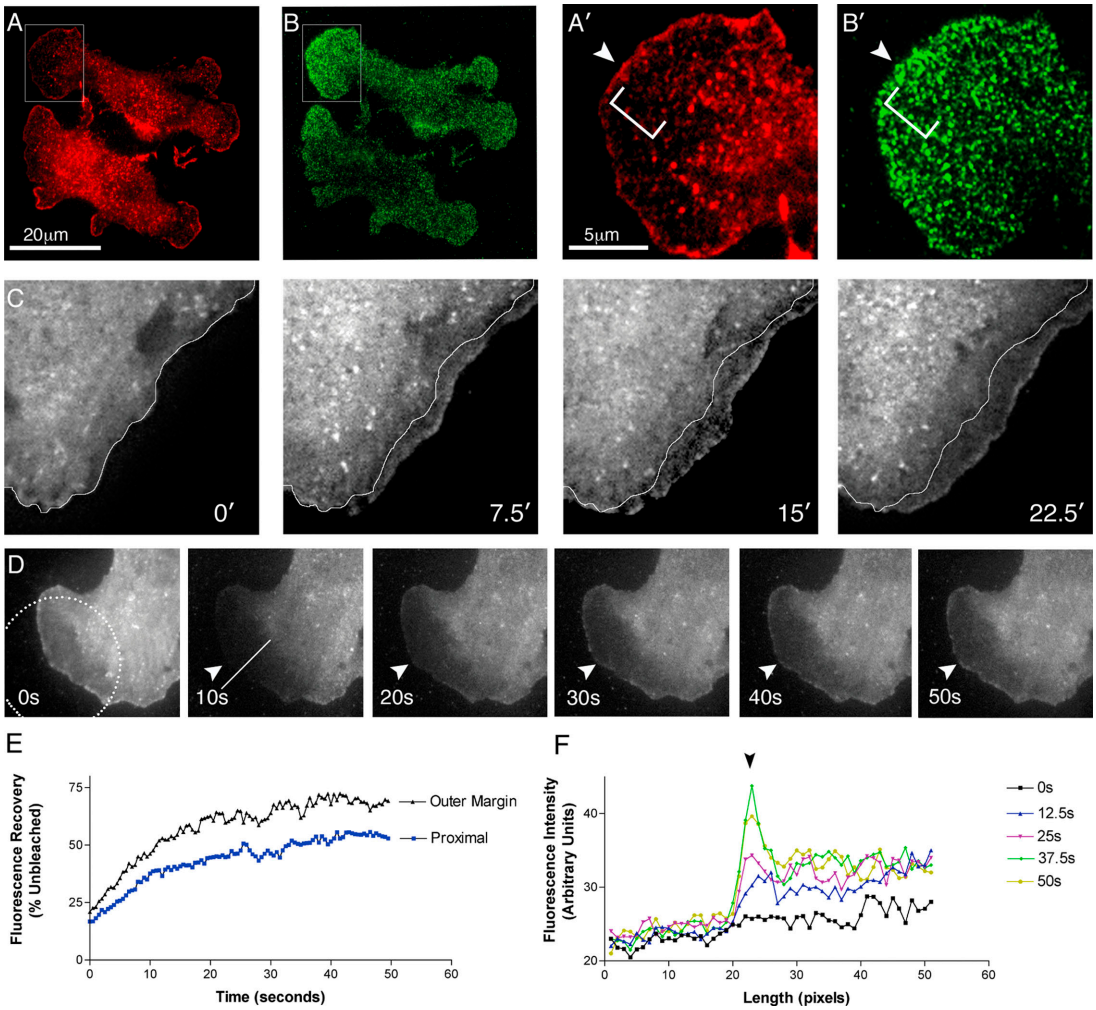

Figure 3. **Cortactin preferentially accumulates at the extending outer margins of cadherin adhesive interfaces.** hE-CHO cells adherent to hE/Fc-coated substrata (60–90 min) were imaged by TIRF microscopy to visualize the cadherin adhesive interface. (A and B) hE-CHO cells were fixed and immunostained for cortactin (A and A′) and β-catenin (B and B′; marking the cadherin–catenin complex). A′ and B′ are higher magnification views of the boxed regions in A and B, respectively. Note that cortactin showed prominent staining at the outer margins of cadherin-based lamellipodia (A and A′, arrowhead), but relative clearing proximal to the outer margins (A′, bracket). In contrast, β-catenin stained in clusters uniformly throughout the contact zone overall (B) and in the cadherin-based lamellipodia (B′). (C) Cortactin accumulates preferentially at the extending outer margin of cadherin-based lamellipodia. Transiently expressed GFP-cortactin was visualized at the adhesive interface of hE-CHO cells adherent to hE/Fc-coated substrata by time-lapse digital TIRF microscopy. Selected frames from Video 1 (available at http://www.jcb.org/cgi/content/full/jcb.200309034/DC1), a representative sequence from three independent experiments, are shown. The outer margin extends progressively during this time sequence (the position of the outer margin in the first frame is marked by the fine lines in subsequent frames). (D–F) Cortactin accumulates preferentially at the outer margin of cadherin-based lamellipodia after fluorescence photobleaching. hE-CHO cells transiently expressing GFP-cortactin were allowed to adhere to hE/Fc-coated substrata for 45 min. The lamellipodia were then photobleached, and fluorescence recovery at the adhesive interface was imaged by time-lapse TIRF microscopy. Data are representative of three independent experiments. (D) A sequence of frames from Video 2 is depicted; the dotted circle identifies the region of photobleaching immediately before photobleaching (0 s), and arrowheads mark the site of the outer margins. (E) Fluorescence recovery occurs more rapidly at outer margins of cadherin-based lamellipodia. Fluorescence intensity in selected regions at the outer margin or proximal lamellipodium was measured in sequential frames after photobleaching (the analyzed regions at the outer margin and proximal lamella are illustrated in Fig. S2, available at http://www.jcb.org/cgi/content/full/jcb.200309034/DC1). At each time point, fluorescence intensities in the selected photobleached areas were normalized to the fluorescence intensities in corresponding regions of identical size (outer margin, proximal lamellipodium) that had not been photobleached. Normalized data are expressed as percentages. (F) Fluorescence intensity profiles of line scans (marked by line in D) through the photobleached area in selected frames after photobleaching. Note that fluorescence recovers progressively throughout the photobleached area, but is most marked as a peak that corresponds to the outer margin (arrowhead). y axis is fluorescence intensity (arbitrary units).

the transgene, accumulation of GFP-cortactin at the outer margins was associated with relative depletion more proximally in the extensions. Thus, cortactin localization at the outer margins appeared to be dynamic, coinciding with outward movement of the outer margin.

This suggested strongly that cortactin might preferentially associate with the outer margins where contact zones were undergoing extension. As a further test of this notion, we used TIRF to assess the patterns of fluorescence recovery in the adhesive interface after photobleaching of GFP-cortac-

tin. As shown in Fig. 3 (D–F) and in Video 2 (available at http://www.jcb.org/cgi/content/full/jcb.200309034/DC1), fluorescence first returned at the very outer margins of the cadherin-based lamellipodia, being readily detectable within 20 s after photobleaching. Measurement of fluorescence intensity showed clear recovery of fluorescence both at the very outer margins and within the lamellipodium proximal to the outer margin itself (Fig. 3 E). However, fluorescence began to increase earlier, and to a greater degree, at the outer margin than in more proximal regions of lamellipodia (Fig. 3 E), suggesting that this was a site for preferential recovery of GFP-cortactin. As a further test, we compared the distribution of fluorescence recovery in line scans through the photobleached area at various times after photobleaching (Fig. 3 F). This analysis showed that although fluorescence progressively increased throughout the photobleached area, recovery was most pronounced at the very outer margin. Together, these data indicate that cortactin accumulated preferentially at the outer margins of cadherin-based lamellipodia where contact zones were being actively extended.

Cortactin localizes with Arp2/3 and participates in actin remodeling at cadherin adhesive contacts

A major target of cortactin is the Arp2/3 actin nucleator complex (Uruno et al., 2001; Weaver et al., 2001). Consistent with this, we found that cortactin colocalized with Arp2/3 at sites of homophilic cadherin adhesion. In bead adhesion assays, cortactin accumulated with transiently expressed GFP-Arp3 at sites of adhesion to hE/Fc-coated beads (Fig. 2 B), but not after binding of Con A–coated beads (unpublished data). In planar spreading assays, cortactin also colocalized precisely with transiently expressed GFP-Arp3 at the outer margins of cadherin-based lamellipodia (Fig. 4). In both these assays, cortactin coaccumulated with F-actin—at the sites of binding to cadherin-coated beads (Fig. 2 B) and in prominent bands at the outer margins of cadherin-based lamellipodia, which we have previously shown to correspond to sites of active actin assembly (Fig. 4; Kovacs et al., 2002b).

To test whether cortactin could participate in actin organization at cadherin adhesive contacts, we examined the effect of cortactin mutants on F-actin accumulation around hE/Fc-coated beads (Fig. 5). When transiently expressed, these cortactin mutants generated polypeptides of the predicted molecular weight and were readily detected by immunofluorescence (Fig. S1, available at http://www.jcb.org/cgi/content/full/jcb.200309034/DC1). F-actin accumulated prominently at the sites of adhesion between control cells and hE/Fc-coated beads (Fig. 5 B; hE/Fc, untransfected). Characteristically, intense F-actin staining was observed in a distinct circumferential pattern around the hE/Fc-coated beads (Fig. 2 and Fig. 5 B). In contrast, no circumferential actin staining was seen upon binding of Con A beads, which showed only occasional actin cables that appeared to originate and terminate in different focal planes than the beads (Fig. 5 B, Con A). Importantly, transient expression of the CA domain of N-WASp (Fig. 5 B, GFP-CA) largely abolished circumferential phalloidin staining around cadherin-coated beads. Because this fragment is a potent inhibitor of Arp2/3 activity (Rohatgi et al., 1999), it indicated that Arp2/3 activity was necessary for cadherin-based actin accumulation upon bead binding.

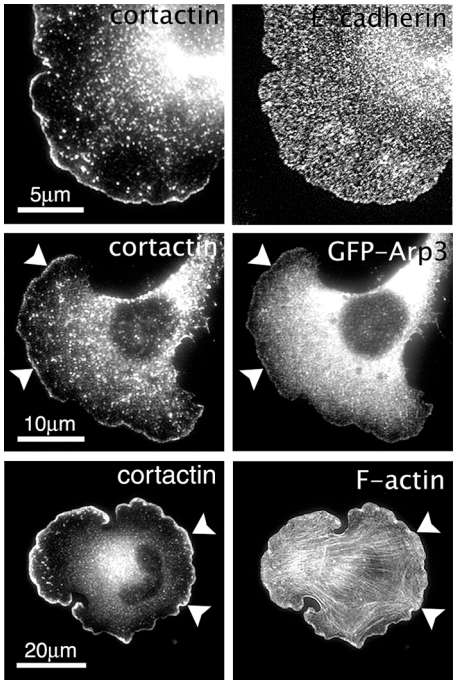

Figure 4. **Cortactin localizes with Arp2/3 at the outer margins of cells adherent to hE/Fc-coated planar substrata.** hE-CHO cells were allowed to adhere to hE/Fc-coated substrata for 90 min, and were then costained for cortactin and cellular E-cadherin, transiently expressed GFP-Arp3, or F-actin, and examined by confocal microscopy. Cortactin colocalized with GFP-Arp3 and F-actin at the outer margins of contact zones (arrowheads).

Circumferential actin accumulation around hE/Fc-beads was also significantly inhibited in cells expressing either cortactin Δ4 (lacking the F-actin–binding site) or cortactin ΔNTA (unable to bind Arp2/3; Fig. 5 B). Semi-quantitative assessment of F-actin accumulation around beads showed that expression of either cortactin mutant inhibited actin accumulation around hE/Fc beads to a similar degree as GFP-CA (Fig. 5 C). In contrast, a mutant in which the three tyrosines phosphorylated by *src* were mutated to phenylalanine (cortactin 3Y, which can inhibit cell motility; Huang et al., 1998) did not affect actin accumulation at cadherin beads. These data strongly suggest that cortactin participates in directing actin assembly at these cadherin contacts, consistent with recent evidence that cortactin participates in Arp2/3-mediated actin assembly (Weaver et al., 2001; Krueger et al., 2003).

Cortactin is functionally important for cadherin contact formation

Actin assembly by Arp2/3 is commonly implicated in generating the forces necessary for cell surface protrusion (Pollard et al., 2000). This led us to test whether cortactin might participate in cadherin-based contact zone extension. First, we examined whether cortactin mutants affected the ability of cells to form cadherin-based lamellipodia using an assay that measures the dimensions of outer margins as a proportion of the total cell periphery (Fig. 6; lamellipodial index, LI). We found that transient expression of mutants that disrupt either the ability of cortactin to bind F-actin (Δ4) or its ability to interact with the Arp2/3 complex (ΔNTA) reduced the

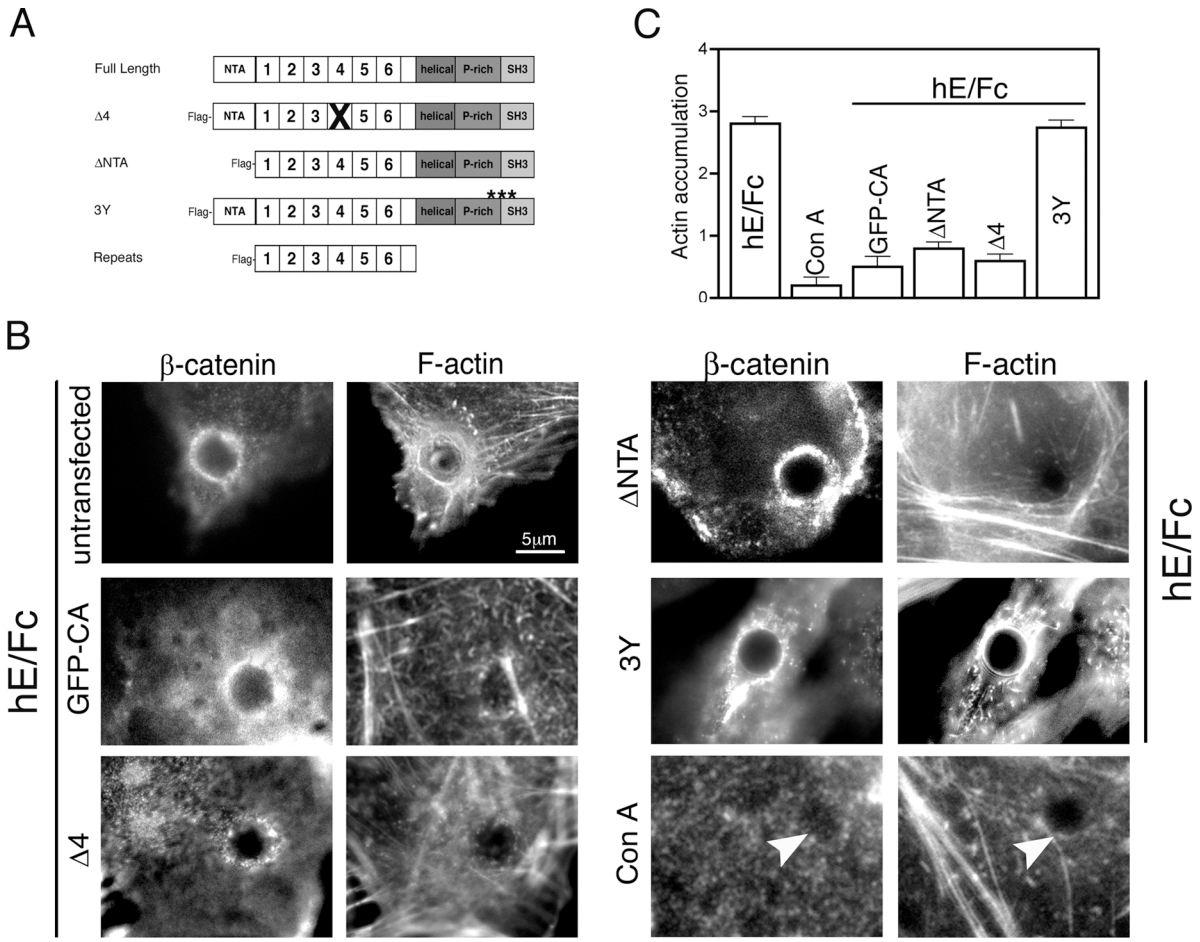

Figure 5. **The actin- and Arp2/3-binding domains of cortactin are required for Arp2/3-dependent actin accumulation stimulated by cadherin ligation.** (A) Schematic of cortactin mutants. The structure of cortactin comprises an NTA region, 6.5 tandem repeats (37 aa each), a helical region (helical), a proline-rich (P-rich) region, and a COOH-terminal SH3 domain. All mutants contained an NH_2-terminal Flag tag. The sites of tyrosines mutated to phenylalanines in the 3Y mutant are marked by asterisks. (B) Immunofluorescence of actin accumulation at cadherin contacts. hE-CHO cells were transiently transfected with either GFP-CA or cortactin mutants Δ4, ΔNTA, or 3Y, and were exposed to hE/Fc- or Con A (arrowheads)–coated beads 24 h later. Transfected cells were examined by triple-label fluorescence microscopy after immunostaining for the appropriate epitope tag (not depicted), β-catenin (marking the cadherin–catenin complex), and F-actin (phalloidin). Representative images are shown. (C) Semiquantitative assessment of phalloidin staining at contacts with hE/Fc-coated beads. Bars are untransfected cells exposed to hE/Fc beads or Con A beads or transfected cells exposed to hE/Fc beads. Data are means ± SEM (n = 30–40 beads analyzed for each test and control).

LI of hE-CHO cells by >50% compared with untransfected controls (Fig. 6). In contrast, neither the 3Y mutant nor a mutant that consisted only of the internal repeats region (Fig. 6, repeats) affected cadherin-based contact zone extension compared with untransfected control cells (Fig. 6).

As an independent loss-of-function approach, we used the pSUPER system for RNA interference (RNAi; Brummelkamp et al., 2002) to suppress cortactin expression. Transient expression of pSUPER-Cort significantly reduced cortactin levels detected in hE-CHO cells by immunoblotting, but did not affect cellular E-cadherin or β-catenin levels (Fig. 7 A). Furthermore, in planar spreading assays, cells with reduced cortactin levels could be clearly detected by immunofluorescence (Fig. 7 B). Cadherin-based lamellipodial extension was reduced by ∼70% in these pSUPER-treated cells compared with control hE-CHO cells cotransfected with an empty pSUPER vector and GFP, which efficiently formed lamellipodia on hE/Fc (Fig. 7 B).

Then, we examined whether cortactin depletion affected the ability of cadherin-containing cells to reform cell–cell contacts after depletion of extracellular calcium (Fig. 8). For these experiments, we used NMuMG mouse epithelial cells that contained endogenous E-cadherin. Although pSUPER-Cort did not produce effective knock-down in these cells, synthetic RNA duplexes reduced cortactin levels by ∼50–60% (Fig. 8 A). Compared with untransfected cells, RNAi-treated cells were significantly slower to reestablish cadherin-based contacts after replacement of extracellular Ca^{2+} (Fig. 8, B and C). Together, these findings demonstrate that cortactin plays an important role in the ability of cells to extend nascent cadherin-based adhesive contacts.

Cortactin participates in the biogenesis of adherens junctions and cell morphology in epithelia

To further assess the function of cortactin, we examined the effects of perturbing cortactin function in MDCK cells, a

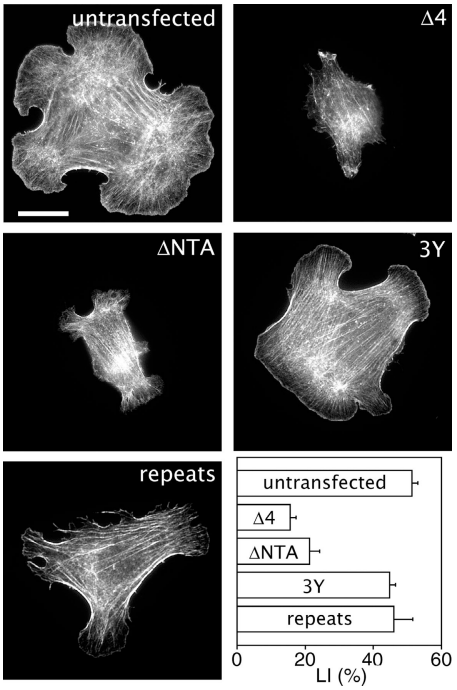

Figure 6. **Cortactin mutants inhibit cadherin-dependent contact zone extension.** hE-CHO cells were transiently transfected with cortactin mutants Δ4, ΔNTA, 3Y, and Repeats. 24 h after transfection, cells were allowed to adhere to hE/Fc-coated substrata for 90 min, fixed, stained with phalloidin, and lamellipodial formation (lamellipodial index, LI) was measured as described in Materials and methods. Representative phalloidin-stained images are shown of cells identified by immunostaining for the Flag epitope tag (not depicted). LI data are means ± SEM (n = 30–50 cells analyzed for each test and controls). Bar, 10 μm.

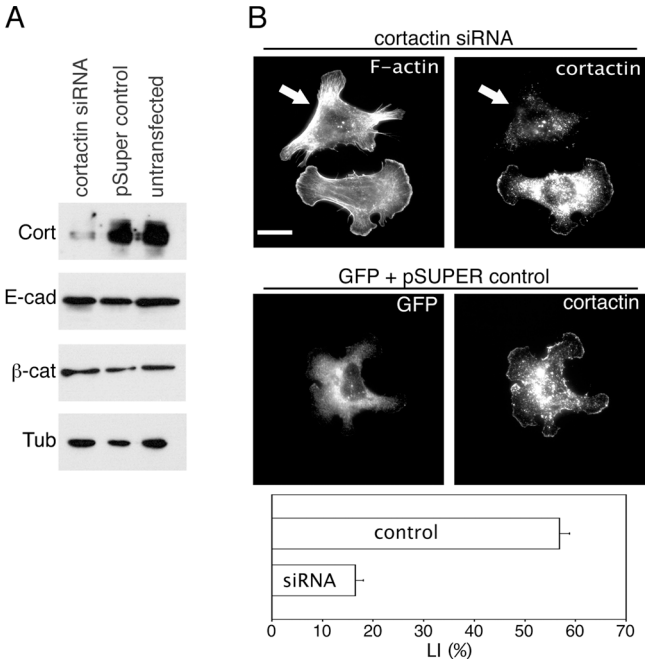

Figure 7. **RNAi-mediated depletion of cortactin inhibits cadherin contact zone extension.** (A) Small interfering RNA depletes cellular cortactin. hE-CHO cells were transiently transfected with pSUPER-Cort or the pSUPER plasmid alone. After 72 h, transfected and untransfected cells were lysed, and proteins were separated by SDS-PAGE and immunoblotted for cortactin (Cort), E-cadherin (E-Cad), β-catenin (β-cat), or tubulin (Tub) as a loading control. (B) RNAi-mediated suppression of endogenous cortactin inhibits cadherin-based lamellipodial formation. hE-CHO cells were analyzed 72 h after transient cotransfection with GFP and either pSUPER-Cort (cortactin siRNA) or the pSUPER plasmid alone (pSUPER control). Transiently transfected hE-CHO cells were allowed to adhere to hE/Fc-coated substrata for 90 min, and cadherin-based lamellipodial formation was measured (lamellipodial index, LI). Transfected cells were identified by coexpression of GFP. Cells were immunostained for endogenous cortactin and F-actin. Note that cells expressing the pSUPER-Cort plasmid (arrows; identified by GFP expression, not depicted) demonstrate less cortactin staining than untransfected cells and a reduced LI compared with control-transfected cells (data are means ± SEM; n = 30–40 cells analyzed for each test and control). Bar, 20 μm.

classic polarized epithelium. Expression of the cortactin Δ4 or ΔNTA mutants dramatically altered cell morphology (Fig. 9). Cells expressing these mutants displayed irregular outlines and long cellular extensions, whereas untransfected cells or cells expressing the vector alone showed the regular cobblestone morphology characteristic of this cell line. Moreover, E-cadherin and β-catenin (unpublished data) failed to accumulate at the sites of contact between these cells and surrounding untransfected cells. In contrast, cells transfected with the Repeats or 3Y cortactin mutants showed no changes in cellular morphology and concentrated E-cadherin in cell–cell contacts, exactly as did control cells.

Cortactin can interact biochemically with the cadherin adhesive complex

As a first step toward characterizing the molecular basis for cortactin recruitment to E-cadherin, we tested the capacity for E-cadherin and cortactin to interact biochemically. As shown in Fig. 10 A, cortactin and E-cadherin coimmunoprecipitated from monolayers of hE-CHO cells, but not from cadherin-negative parental CHO cells. Cortactin also coimmunoprecipitated E-cadherin from MDCK cell monolayers, both before and during recovery after depletion of extracellular Ca^{2+} (Fig. 10 B).

Further, we found that E-cadherin coimmunoprecipitated from hE-CHO cells plated onto hE/Fc, but not from cells plated onto poly-L-lysine (Fig. 10 C), suggesting that sustained cadherin ligation was sufficient to cause cortactin and E-cadherin to interact biochemically. We estimate that ~1–2% of total cellular E-cadherin was found in the cortactin immunoprecipitates (Fig. 10 C). However, this is likely to significantly underestimate the true stoichiometry of the cortactin–cadherin interaction because the cortactin immunoprecipitates probably contain a significant amount of cortactin not complexed with cadherin. Finally, the association between cortactin and E-cadherin did not depend on actin filament integrity because the efficiency of coimmunoprecipitation was unaffected by latrunculin A (Fig. 10 D) added to the intact cells or after lysis.

Discussion

It is increasingly apparent that key aspects of cadherin biology entail close functional cooperation between the surface-

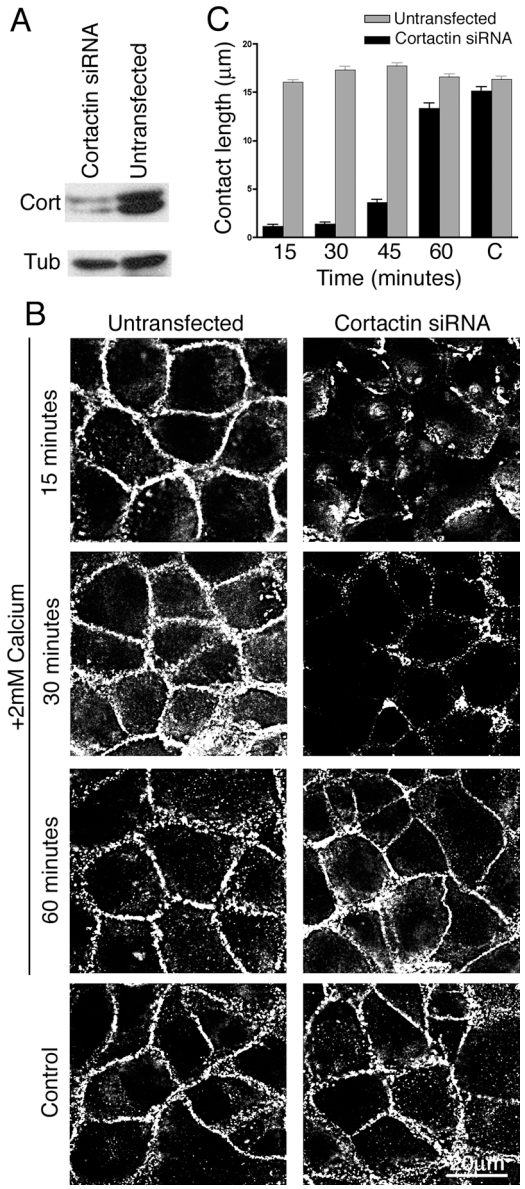

Figure 8. **Cortactin is necessary for the efficient formation of native cell–cell contacts.** NMuMG mouse epithelial cells were transfected with synthetic cortactin RNA duplexes and studied 48 h after transfection. (A) Immunoblotting of cell lysates for cortactin or tubulin (as a loading control) showed efficient depletion of endogenous cortactin in RNAi-treated cells. (B and C) The ability of cells to reform contacts was assessed after chelation of extracellular calcium. Untransfected and RNAi-treated cultures were fixed at 15–60 min after restoration of extracellular calcium, and were compared with monolayers maintained in the continuous presence of Ca^{2+} (Control). (B) Representative epi-illumination images of untransfected and RNAi-treated cultures stained for E-cadherin. Although control cells had substantially reformed cadherin-containing contacts within 15 min of replacing extracellular Ca^{2+}, RNAi-treated cells were significantly delayed in reforming contacts. (C) Reassembly of contacts was quantitated by measuring the lengths of individual cadherin-containing cell–cell contacts. Data are means ± SEM (n = 250–320).

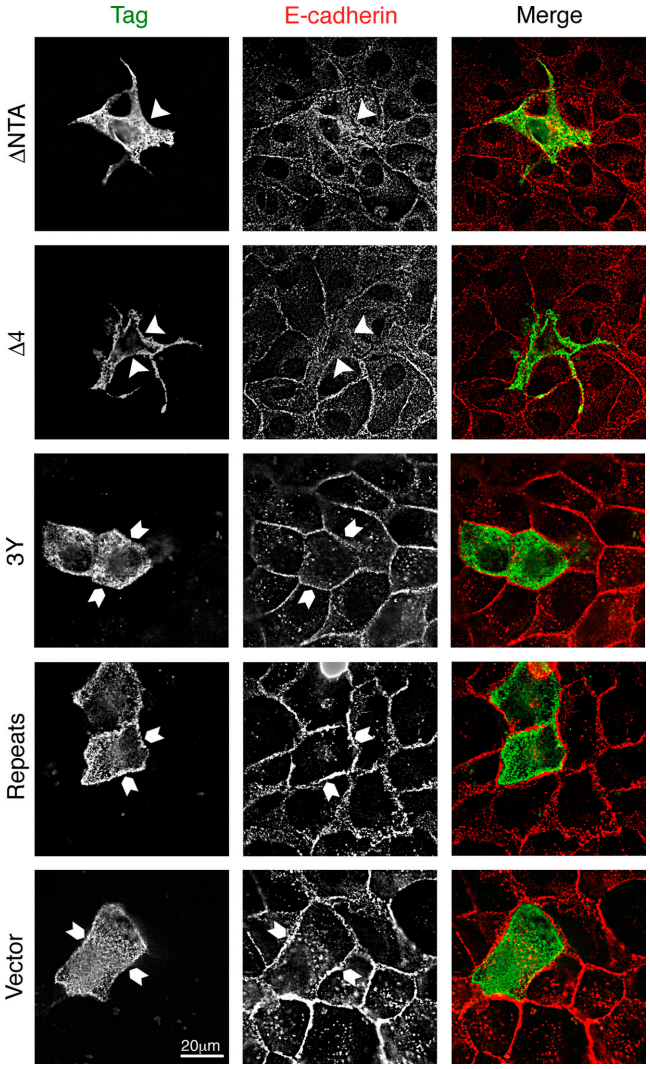

Figure 9. **Cortactin mutants perturb junctional biogenesis and cell morphology in polarized epithelial monolayers.** Near-confluent MDCK cell cultures were transiently transfected with cortactin mutants ΔNTA, Δ4, 3Y, and Repeats, or with a control vector expressing GFP alone. After 24 h, cultures were fixed and immunostained for the epitope tag and E-cadherin (DECMA-1). Epi-illumination fluorescence images were processed by three-dimensional blind deconvolution from z-axis stacks. Although cells expressing 3Y, Repeats, or GFP alone showed regular epithelioid morphology and accumulate E-cadherin in junctions (chevrons), cells expressing either the Δ4 or ΔNTA mutants showed gross disturbances in cell morphology and failed to concentrate E-cadherin in contacts (arrowheads).

adhesive action of cadherin molecules and the force-generating capacity of actin assembly. Our current data identify a necessary role for cortactin in this cooperation, based on four observations: (1) cortactin and Arp2/3 coaccumulated in dynamic cadherin contacts, notably those at the outer margins of extending contact zones; (2) cortactin mutants effectively inhibited F-actin accumulation in cadherin contacts, a process that requires Arp2/3 activity; and (3) perturbing cortactin function profoundly affected the ability of cells to extend cadherin-adhesive contacts and (4) disturbed the biogenesis of adherens junctions in MDCK cells, accompanied by gross distortions of epithelial cell morphology.

Actin assembly has the capacity both to drive cell surfaces together to initiate contacts (Vasioukhin et al., 2000) and to promote extension of cadherin-based cell contacts upon one another after contacts are first made (Kovacs et al., 2002b).

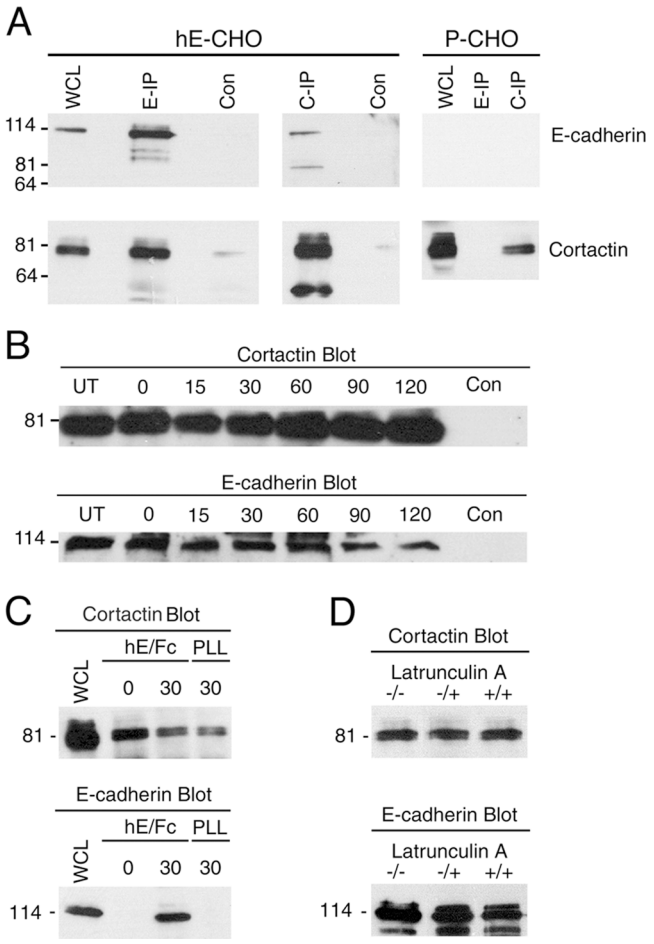

Figure 10. **Cortactin associates with the E-cadherin adhesion complex.** (A) Cellular E-cadherin coimmunoprecipitates with cortactin. Protein complexes were immunoprecipitated from monolayers of hE-CHO cells (hE-CHO) or untransfected parental CHO cells (P-CHO) using either a polyclonal anti-E-cadherin antibody (E-IP) or an anti-cortactin antibody (pAb C2; C-IP). Immunoprecipitates and whole-cell lysates (WCL) were separated by SDS-PAGE and were then immunoblotted for E-cadherin (E-cad; mAb HECD-1) or cortactin (Cort; mAb 4F11). Negative controls for immunoprecipitations were nonimmune antisera (Con). The bottom bands are degradation products. (B) Cortactin associates with E-cadherin during assembly of cell–cell contacts. Cortactin was immunoprecipitated (pAb C2) from MDCK lysates prepared from untreated monolayers (UT), immediately after incubation with 2 mM EGTA (0) or 15–120 min after replacing extracellular Ca^{2+}. Immune complexes were probed for cortactin (mAb 4F11) or E-cadherin (mAb 3B8). A naive rabbit antiserum was used as a negative control (Con). (C) Cortactin associates with E-cadherin in a ligation-dependent fashion. Cortactin was immunoprecipitated (pAb C2) from freshly isolated hE-CHO cells (time 0) or from hE-CHO cells after a 30-min adhesion to substrata coated with either hE/Fc or poly-L-lysine (PLL). Immune complexes were separated by SDS-PAGE and immunoblotted for either cortactin or E-cadherin. (D) The association between E-cadherin and cortactin does not depend on actin filament integrity. Anti-E-cadherin immune complexes were isolated from (1) lysates of hE-CHO cell monolayers that were untreated (−/−); (2) lysates that included 1 μM latrunculin A added to the lysis buffer (−/+); and (3) lysates of cells pretreated with 1 μM latrunculin A for 15 min before lysis (as well as having latrunculin also included in the lysis buffer; +/+). This treatment with latrunculin A was sufficient to disrupt phalloidin staining patterns in the cells (not depicted). Western blots were probed for both cortactin and E-cadherin.

In the latter case, E-cadherin ligation itself is likely to be an active participant, by directing where actin assembly concentrates in contact zones. We found that cortactin mutants profoundly inhibit actin accumulation at adhesive contacts with cadherin-coated beads. We chose to use bead assays in these experiments because they provide spatially defined, cadherin-specific adhesive cues that are independent of cell spreading. Similar approaches demonstrated that G-actin incorporates at the adhesive contact with N-cadherin–coated beads (Lambert et al., 2002), and we confirmed that F-actin accumulation at bead adhesions was inhibited by an N-WASp fragment that effectively inhibits Arp2/3-mediated actin assembly in vitro (Rohatgi et al., 1999). Therefore, our results suggest strongly that cortactin activity is necessary for the Arp2/3-dependent actin assembly that occurs in response to E-cadherin homophilic ligation.

In keeping with a role for actin assembly in extending adhesive contacts, we found that the ability of cells to extend cadherin contacts in planar spreading assays was dramatically reduced when cortactin activity was perturbed, either by expression of dominant-negative cortactin mutants or by RNAi-mediated knock-down of endogenous cortactin. Furthermore, depletion of cortactin in NMuMG cells significantly reduced the efficiency with which cells reestablished contacts with one another. Together, these findings indicate that cortactin plays a key role in cadherin-based contact zone extension. In separate analyses, we also recently established that Arp2/3 activity is necessary for extension of cadherin adhesive contacts in these assays (unpublished data). Thus, we interpret these findings to indicate that cortactin is necessary for Arp2/3-mediated actin assembly to effectively drive cell surfaces together during contact zone extension.

In vitro, cortactin can increase net actin assembly by directly or indirectly stimulating the catalytic activity of the Arp2/3 complex (Uruno et al., 2001; Weaver et al., 2001, 2002), as well as stabilizing actin filaments at a post-nucleation step (Weaver et al., 2001). Any of these actions, individually or in concert, may account for the contribution of cortactin to the cadherin-mediated actin assembly that we observed. Notably, our analysis of cortactin mutants suggests that both the Arp2/3-binding and F-actin–binding domains of the molecule are necessary for actin assembly at cadherin contacts. Hence, the ability of cortactin to act as a multidomain scaffold, simultaneously linking Arp2/3 and actin filaments, may be a key to its role in cadherin-directed actin assembly. The inhibitory effect of the cortactin ΔNTA mutant might then be explained by its ability to displace endogenous cortactin from filaments (because this mutant retains the F-actin–binding site), whereas the Δ4 mutant would compete with endogenous cortactin for Arp2/3, but be incapable of binding F-actin.

Ultimately, for cortactin to potentiate Arp2/3 activity, this protein must also be strictly recruited to sites of actin assembly at the cell surface. Indeed, we found that cortactin colocalizes with the Arp2/3 complex exactly where cadherin adhesion induces actin assembly—around nascent contacts with cadherin-coated beads and at the outer margins of contact zones in planar adhesion assays. Furthermore, after photobleaching, GFP-cortactin appeared to preferentially re-

cruit to the outer margins of cadherin-based lamellipodia where contact zones were being actively extended (Kovacs et al., 2002b). Such selective accumulation might reflect either preferential delivery of cortactin to these regions and/or selective retention at these sites. Irrespective of the mechanism, this finding indicates that cortactin is recruited to specific subregions within individual cadherin contacts, suggesting that the adhesive contact zones are not biochemically or functionally uniform structures (Ehrlich et al., 2002; Kovacs et al., 2002b).

Our data further indicate that cortactin recruitment occurs as a consequence of cadherin homophilic ligation and, indeed, is associated with a biochemical interaction between cortactin and the cadherin adhesive complex. Most notably, presentation of a cadherin-specific adhesive signal (on beads or planar substrata) was sufficient to recruit cortactin to adhesive sites and induce cortactin to coimmunoprecipitate with E-cadherin. In contrast, nonspecific adhesive ligands did not recruit cortactin to the membrane, nor did they allow the cadherin–cortactin biochemical interaction to be sustained.

Although we have yet to elucidate the molecular mechanism that links cortactin to the cadherin adhesive complex, our data argue against it being a constitutive interaction. In planar spreading assays, much E-cadherin did not colocalize with cortactin, and in our current experiments only a small proportion of total cellular E-cadherin was found in the cortactin immunoprecipitates. Similarly, integrin-based cell migration also entails a functionally important interaction between small subpopulations of Arp2/3 and vinculin (DeMali et al., 2002). Although cortactin may interact with some members of the p120-catenin family (Martinez et al., 2003), this suggests that the contribution of cortactin to cadherin function involves a specific pool of cadherin molecules, presumably that is responsible for recruiting Arp2/3. Similarly, we observed earlier that only a subpopulation of the cellular pools of cadherin and Arp2/3 interacted biochemically during contact extension (Kovacs et al., 2002b).

Instead, it is likely that recruitment of cortactin to cadherin contacts is signal regulated, consistent with emerging evidence that multiple signals determine both Arp2/3 activity (Machesky and Insall, 1999) and cortactin localization (Head et al., 2003). A good candidate here is Rac, which clearly stimulates cortactin recruitment in motile cells (Weed et al., 1998). Moreover, Rac is directly activated by cadherin ligation (Nakagawa et al., 2001; Kovacs et al., 2002a), and is likely to be spatially confined to the outer margins in extending contact zones (Ehrlich et al., 2002; Kovacs et al., 2002a), exactly corresponding to the sites where cortactin recruits in our analyses. Spatio-temporal localization of signals may then be an important factor that directs cortactin to specific subregions within individual adhesive contact zones.

In summary, we have identified cortactin as a novel determinant of cadherin–actin cooperativity during adhesive contact formation. We envisage that cortactin acts in newly forming contacts to promote Arp2/3-mediated cell surface protrusion, thereby driving the extension of nascent contacts to form stable zones of adhesion. However, the impact of cortactin is not confined to the early stages of contact formation. Cortactin mutants significantly inhibited the accumulation of E-cadherin in contacts between MDCK cells, a hallmark of adherens junctions assembly, accompanied by gross distortions of epithelial cell morphology (residual cortactin likely explains why morphologic changes were less apparent in RNAi-treated NMuMG cells). Interestingly, the cortactin mutants that most effectively perturbed cadherin-directed actin assembly and contact zone extension (Δ4 and ΔNTA) were also the most potent in disrupting junctional assembly and epithelial morphology. These effects of cortactin on later stages of epithelial biogenesis may therefore reflect a requirement for efficient contact zone extension early in the process of contact formation. However, cortactin may also participate in other aspects of junctional biogenesis. For example, cortactin also binds directly to ZO-1, a cytoplasmic scaffolding protein of the tight junction in both invertebrate and vertebrate cells (unpublished data; Katsube et al., 1998), which can also associate with adherens junctions. Given its potential to support multiple intermolecular interactions (Weed and Parsons, 2001), cortactin may then act as a signal integrator in cadherin contacts, coupling adhesion to actin dynamics, cell signaling, and junctional assembly.

Materials and methods

Cell culture, transfections, and hE/Fc

hE-CHO cells, hE/Fc purification, and preparation of hE/Fc-coated substrata and latex beads (6-μm-diam) have been described previously (Kovacs et al., 2002a,b). Transient transfections were performed with LipofectAMINE™ (Invitrogen) according to the manufacturer's instructions. MDCK cells were cultured in DME with 10% FCS and 2 mM glutamine; NMuMG cells in DME with 10% FBS and 10 μg/ml insulin.

Antibodies

Primary antibodies were as follows: (1) a pAb directed against the ectodomain of human E-cadherin was raised in rabbits using hE/Fc as an immunogen. In Western blots, this pAb recognized a single 116-kD polypeptide band in lysates from MCF-7 and hE-CHO cells, but not in lysates from parental CHO cells that lack E-cadherin; (2) mouse mAb against the cytoplasmic tail of human E-cadherin (Transduction Laboratories); (3) mAb HECD1 against human E-cadherin (provided by Dr. M. Wheelock [University of Nebraska, Omaha, NE], with the permission of Dr. M. Takeichi [RIKEN CDB, Kobe, Japan]); (4) mouse mAb 3B8 directed against canine E-cadherin (a gift from Dr. Warren Gallin, University of Alberta, Edmonton, Alberta, Canada); (5) rat mAb DECMA-1 against mouse E-cadherin (Sigma-Aldrich); (6) rabbit pAb against the NH_2 terminus of *Xenopus* β-catenin (a gift of Dr. Barry Gumbiner, University of Virginia, Charlottesville, VA); (7) mouse mAb 4F11 against cortactin (Wu et al., 1991); (8) rabbit pAb C2 raised against chicken cortactin; (9) anti-FLAG mAb M5 (Sigma-Aldrich); (10) rabbit anti-GFP pAb (Molecular Probes, Inc.); and (11) anti-GFP mAb (Roche). F-actin was identified using Alexa® 488– or Alexa® 568–labeled phalloidin (Molecular Probes, Inc.). Secondary antibodies were species-specific antibodies conjugated with Alexa® 350, Alexa® 488, or Texas red (Molecular Probes, Inc.).

Plasmids

The pEGFP-CA construct bearing the CA fragment of N-WASp was a gift of Drs. H. Miki and T. Takenawa (University of Tokyo, Tokyo, Japan). GFP-Arp3 (constructed by Dr. Matt Welch) was a gift from Dr. D. Schaefer (Washington University, St. Louis, MO). GFP-cortactin and the cortactin mutants Δ4, Repeats, and 3Y were described earlier (Weed et al., 2000; Kinley et al., 2003). The cortactin ΔNTA expression construct was created by PCR amplification of mp85.L7 (Miglarese et al., 1994), with a 5′ primer flanking codon 85 containing a KpnI restriction site and a 3′ primer flanking the stop codon (546) containing an EcoRI restriction site. The amplified PCR product was digested with KpnI and EcoRI and subcloned in frame into KpnI–EcoRI-digested pcDNA3FLAG2AB. The final construct was tested by DNA sequencing.

To generate the pSUPER-Cort construct, the pSUPER vector was digested with BglII and HindIII and then ligated with the annealed oligonu-

cleotides 5′-gatccccCACATCAACATTCACAAGCttcaagagaGCTTGTGAATGTTGATGTGtttttggaaa-3′ and 5′-agcttttccaaaaaCACATCAACATTCACAAGCtctcttgaaGCTTGTGAATGTTGATGTGggg-3′ (cortactin sequences are in uppercase, corresponding to bases 284–302 in the murine cortactin cDNA; Miglarese et al., 1994). Oligonucleotides were HPLC purified and 5′-phosphorylated before annealing. The pSUPER-Cort sequence was verified by DNA sequencing.

Synthetic RNA duplexes based on the sequences 5′-AAAGCTTCGAGAGAATGTCTT-3′ and 5′-AAGACTGAGAAGCATGCCTCC-3′ were prepared using the Silencer™ kit (Ambion). Cells were transfected with a cocktail of both duplexes using siPORT™ Amine (Ambion) as per the manufacturer's instructions.

Immunofluorescence microscopy and quantitation

Samples were prepared for immunofluorescence analysis as described previously (Kovacs et al., 2002a,b). Fixed material was mounted in 1% *N*-propyl-gallate in 50% glycerol:PBS for epi-illumination and laser-scanning confocal microscopy; glycerol was omitted from the mounting medium for TIRF. Fixed material was examined by epi-illumination using microscopes (model AX70 or IX81; Olympus) with 60×, 1.4 NA or 100×, 1.4 NA objectives (Olympus), and was imaged with cameras (Orca 1 or Orca-ER; Hamamatsu). TIRF imaging was performed using a microscope (model IX81; Olympus) and an objective (60×, 1.45 NA; Olympus) illuminated with a 10-mW argon laser. For live-cell imaging, cells were incubated in phenol red–free HBSS at 37°C. All acquisition and movies were controlled using MetaMorph® software (Universal Imaging Corp.). Photobleaching was performed by closing the iris field diaphragm in the epi-illumination pathway and illuminating with a 100-W Hg lamp for 10 s. Laser-scanning confocal microscopy was performed using a scanning system (MRC 600; Bio-Rad Laboratories) mounted on a microscope (Axioskop; Carl Zeiss MicroImaging, Inc.) equipped with a Plan-Apochromat 63× objective (Carl Zeiss MicroImaging, Inc.) running under Bio-Rad Laboratories software. Some epi-illumination images were deconvolved from z-stacks using three-dimensional blind deconvolution (Autoquant). Movie images were compiled and converted to QuickTime stacks using ImageJ. Figures were assembled for presentation in Adobe Photoshop®.

To quantitate cadherin-based contact formation in planar spreading assays, phalloidin-stained images were analyzed using MetaMorph® software. For each cell, the lamellipodial index was calculated as follows: lamellipodial outer margins were identified by their broad phalloidin staining, were measured, and the total length of outer margins in each cell was expressed as a percentage of the cell perimeter for that cell. Contact formation in calcium jump experiments was quantitated by measuring the lengths of individual cadherin contacts (defined as lines of continuous cadherin staining between cell vertices). As a semiquantitative estimate of actin accumulation around hE/Fc-coated beads, the degree of phalloidin staining around beads was assessed using a scoring system based on the proportion of the circumference of the bead showing intense F-actin accumulation. 4+, complete circumferential F-actin accumulation; 3+, ∼75% of the perimeter; 2+, ∼50% perimeter; 1+, ∼25%; 0, no actin accumulation.

Immunoprecipitations

Cells were lysed in 1 ml lysis buffer (1% NP-40, 150 mM NaCl, 50 mM Tris-HCl, pH 7.4, 1 mM EDTA, 50 mM NaF, 2 mM sodium vanadate, 0.1% BSA, and complete protease inhibitors [Roche]). Protein complexes were immunoprecipitated with either a polyclonal E-cadherin antibody or a C2 pAb directed against cortactin bound to protein A–agarose beads and were separated by SDS-PAGE. Immune complexes were blotted for E-cadherin and cortactin. Blots were scanned and compiled in Adobe Photoshop® (v. 6).

Online supplemental material

Online supplemental material includes expression characterization of the cortactin mutants used in this work (Fig. S1), graphical illustration of the regions chosen to analyze FRAP (Fig. S2), and the videos of GFP-cortactin localization imaged by TIRF (Videos 1 and 2) that are illustrated in Fig. 3. Online supplemental material available at http://www.jcb.org/cgi/content/full/jcb.200309034/DC1.

We thank all our aforementioned colleagues for the gifts of antibodies and reagents; Drs. Tom Fleming and Bhav Seth for sharing unpublished data; Dr. Joe Loureiro for critical reading of the manuscript; Julie Head for her assistance in generating and validating cortactin plasmids; Roger Daly, Gillian Lehrbach, and the Garvan Institute Cell Culture facility (Sydney, Australia) for NMuMG cells; Teresa Munchow for assiduous tissue culture support; Sandrine Roy for transfection advice; and all our colleagues in the lab for their support, encouragement, and advice.

The work in Australia was supported by grants to A.S. Yap from the National Health and Medical Research Council (Australia), Wellcome Trust, and Human Frontiers Science Program. S.A. Weed is supported by grant K22 DE 14364 from the National Institute of Dental and Craniofacial Research. Support is also provided by a grant from the National Institute of Diabetes and Digestive and Kidney Diseases (RO1 DK061397) to A.S. Fanning and James M. Anderson; and A.S. Yap is a Wellcome Trust Senior International Medical Research Fellow.

Submitted: 5 September 2003
Accepted: 15 January 2004

References

Adams, C.L., and W.J. Nelson. 1998. Cytomechanics of cadherin-mediated cell-cell adhesion. *Curr. Opin. Cell Biol.* 10:572–577.

Adams, C.L., Y.-T. Chen, S.J. Smith, and W.J. Nelson. 1998. Mechanisms of epithelial cell-cell adhesion and cell compaction revealed by high-resolution tracking of E-cadherin-green fluorescent protein. *J. Cell Biol.* 142:1105–1119.

Brummelkamp, T.R., R. Bernards, and R. Agami. 2002. A system for stable expression of short interfering RNAs in mammalian cells. *Science.* 296:550–553.

DeMali, K.A., C.A. Barlow, and K. Burridge. 2002. Recruitment of the Arp2/3 complex to vinculin: coupling membrane protrusion to matrix adhesion. *J. Cell Biol.* 159:881–891.

Ehrlich, J.S., M.D. Hansen, and W.J. Nelson. 2002. Spatio-temporal regulation of Rac1 localization and lamellipodia dynamics during epithelial cell-cell adhesion. *Dev. Cell.* 3:259–270.

Goodwin, M., E.M. Kovacs, M.A. Thoreson, A.B. Reynolds, and A.S. Yap. 2003. Minimal mutation of the cytoplasmic tail inhibits the ability of E-cadherin to activate Rac but not phosphatidylinositol 3-kinase: direct evidence of a role for cadherin-activated Rac signaling in adhesion and contact formation. *J. Biol. Chem.* 278:20533–20539.

Head, J.A., D. Jiang, M. Li, L.J. Zorn, E.M. Schaefer, J.T. Parsons, and S.A. Weed. 2003. Cortactin tyrosine phosphorylation requires Rac1 activity and association with the cortical actin cytoskeleton. *Mol. Biol. Cell.* 14:3216–3229.

Higgs, H.N. 2002. Actin nucleation: cortactin caught in the act. *Curr. Biol.* 12: R593–R595.

Huang, C., J. Liu, C.C. Haudenschild, and X. Zhan. 1998. The role of tyrosine phosphorylation of cortactin in the locomotion of endothelial cells. *J. Biol. Chem.* 273:25770–25776.

Kaksonen, M., H.B. Peng, and H. Rauvala. 2000. Association of cortactin with dynamic actin in lamellipodia and on endosomal vesicles. *J. Cell Sci.* 113: 4421–4426.

Katsube, T., M. Takahisa, R. Ueda, N. Hashimoto, M. Kobayashi, and S. Togashi. 1998. Cortactin associates with the cell-cell junction protein ZO-1 in both Drosophila and mouse. *J. Biol. Chem.* 273:29672–29677.

Kinley, A.W., S.A. Weed, A.M. Weaver, A.V. Karginov, E. Bissonette, J.A. Cooper, and J.T. Parsons. 2003. Cortactin interacts with WIP in regulating Arp2/3 activation and membrane protrusion. *Curr. Biol.* 13:384–393.

Kovacs, E.M., R.G. Ali, A.J. McCormack, and A.S. Yap. 2002a. E-cadherin homophilic ligation directly signals through Rac and PI3-kinase to regulate adhesive contacts. *J. Biol. Chem.* 277:6708–6718.

Kovacs, E.M., M. Goodwin, R.G. Ali, A.D. Paterson, and A.S. Yap. 2002b. Cadherin-directed actin assembly: E-cadherin physically associates with the Arp2/3 complex to direct actin assembly in nascent adhesive contacts. *Curr. Biol.* 12:379–382.

Krueger, E.W., J.D. Orth, H. Cao, and M. McNiven. 2003. A dynamin-cortactin-Arp2/3 complex mediates actin reorganization in growth factor-stimulated cells. *Mol. Biol. Cell.* 14:1085–1096.

Lambert, M., D. Choquet, and R.M. Mege. 2002. Dynamics of ligand-induced, Rac1-dependent anchoring of cadherins to the actin cytoskeleton. *J. Cell Biol.* 157:469–479.

Lynch, D.K., S.C. Winata, R.J. Lyons, W.E. Hughes, G.M. Lehrbach, V. Wasinger, G. Corthals, S. Cordwell, and R.J. Daly. 2003. A cortactin-CD2-associated protein (CD2AP) complex provides a novel link between epidermal growth factor receptor endocytosis and the actin cytoskeleton. *J. Biol. Chem.* 278:21805–21813.

Machesky, L.M., and R.H. Insall. 1999. Signaling to actin dynamics. *J. Cell Biol.* 146:267–272.

Martinez, M.C., T. Ochiishi, M. Majewski, and K.S. Kosik. 2003. Dual regulation of neuronal morphogenesis by a delta-catenin-cortactin complex and Rho. *J. Cell Biol.* 162:99–111.

Miglarese, M.R., J. Mannion-Henderson, H. Wu, J.T. Parsons, and T.P. Bender.

1994. The protein tyrosine kinase substrate cortactin is differentially expressed in murine B lymphoid tumors. *Oncogene.* 9:1989–1997.

Nakagawa, M., M. Fukata, M. Yamagawa, M. Itoh, and K. Kaibuchi. 2001. Recruitment and activation of Rac1 by the formation of E-cadherin-mediated cell-cell adhesion sites. *J. Cell Sci.* 114:1829–1838.

Noren, N.K., C.M. Niessen, B.M. Gumbiner, and K. Burridge. 2001. Cadherin engagement regulates Rho family GTPases. *J. Biol. Chem.* 276:33305–33308.

Olazabal, I.M., and L.M. Machesky. 2001. Abp1p and cortactin, new "handholds" for actin. *J. Cell Biol.* 154:679–682.

Pollard, T.D., L. Blanchoin, and R.D. Mullins. 2000. Molecular mechanisms controlling actin filament dynamics in nonmuscle cells. *Annu. Rev. Biophys. Biomol. Struct.* 29:545–576.

Rohatgi, R., L. Ma, H. Miki, M. Lopez, T. Kirchhausen, T. Takenawa, and M.W. Kirschner. 1999. The interaction between N-WASP and the Arp2/3 complex links Cdc42-dependent signals to actin assembly. *Cell.* 97:221–231.

Steyer, J.A., and W. Almers. 2001. A real-time view of life within 100 nm of the plasma membrane. *Nat. Rev. Mol. Cell Biol.* 2:268–275.

Takeichi, M. 1991. Cadherin cell adhesion receptors as a morphogenetic regulator. *Science.* 251:1451–1455.

Uruno, T., J. Liu, P. Zhang, Y.-X. Fan, C. Egile, R. Li, S.C. Mueller, and X. Zhan. 2001. Activation of Arp2/3 complex-mediated actin polymerization by cortactin. *Nat. Cell Biol.* 3:259–266.

Vaezi, A., C. Bauer, V. Vasioukhin, and E. Fuchs. 2002. Actin cable dynamics and Rho/Rock orchestrate a polarized cytoskeletal architecture in the early steps of assembling a stratified epithelium. *Dev. Cell.* 3:367–381.

Vasioukhin, V., C. Bauer, M. Yin, and E. Fuchs. 2000. Directed actin polymerization is the driving force for epithelial cell-cell adhesion. *Cell.* 100:209–219.

Weaver, A.M., A.V. Karginov, A.W. Kinley, S.A. Weed, Y. Li, J.T. Parsons, and J.A. Cooper. 2001. Cortactin promotes and stabilizes Arp2/3-induced actin filament network formation. *Curr. Biol.* 11:370–374.

Weaver, A.M., J.E. Heuser, A.V. Karginov, W.-L. Lee, J.T. Parsons, and J.A. Cooper. 2002. Interaction of cortactin and N-WASp with Arp2/3 complex. *Curr. Biol.* 12:1270–1278.

Weed, S.A., and J.T. Parsons. 2001. Cortactin: coupling membrane dynamics to cortical actin assembly. *Oncogene.* 20:6418–6434.

Weed, S.A., Y. Du, and J.T. Parsons. 1998. Translocation of cortactin to the cell periphery is mediated by the small GTPase Rac1. *J. Cell Sci.* 111:2433–2443.

Weed, S.A., A.V. Karginov, D.A. Schafer, A.M. Weaver, A.W. Kinley, J.A. Cooper, and J.T. Parsons. 2000. Cortactin localization to sites of actin assembly in lamellipodia requires interactions with F-actin and the Arp2/3 complex. *J. Cell Biol.* 151:29–40.

Wu, H., and J.T. Parsons. 1993. Cortactin, an 80/85-kilodalton pp60src substrate, is a filamentous actin-binding protein enriched in the cell cortex. *J. Cell Biol.* 120:1417–1426.

Wu, H., A.B. Reynolds, S.B. Kanner, R.R. Vines, and J.T. Parsons. 1991. Identification and characterization of a novel cytoskeleton-associated pp60src substrate. *Mol. Cell. Biol.* 11:5113–5124.

Yap, A.S., and E.M. Kovacs. 2003. Direct cadherin-activated cell signaling: a view from the plasma membrane. *J. Cell Biol.* 160:11–16.

Yap, A.S., W.M. Brieher, and B.M. Gumbiner. 1997. Molecular and functional analysis of cadherin-based adherens junctions. *Annu. Rev. Cell Dev. Biol.* 13: 119–146.